

4-Alkyl-1,2,4-triazole-3-thione analogues as metallo- $\beta$ -lactamase inhibitors

Laurent Gavara<sup>a,\*</sup>, Alice Legru<sup>a</sup>, Federica Verdirosa<sup>b</sup>, Laurent Seville<sup>a</sup>, Lionel Nauton<sup>c</sup>,  
Giuseppina Corsica<sup>b</sup>, Paola Sandra Mercuri<sup>d</sup>, Filomena Sannio<sup>b</sup>, Georges Feller<sup>e</sup>,  
Rémi Coulon<sup>a</sup>, Filomena De Luca<sup>b</sup>, Giulia Cerboni<sup>b</sup>, Silvia Tanfoni<sup>b</sup>, Giulia Chelini<sup>b</sup>,  
Moreno Galleni<sup>d</sup>, Jean-Denis Docquier<sup>b,f,\*</sup>, Jean-François Hernandez<sup>a,\*</sup>

<sup>a</sup> Institut des Biomolécules Max Mousseron, UMR5247 CNRS, Université de Montpellier, ENSCM, Faculté de Pharmacie, 34093 Montpellier Cedex 5, France

<sup>b</sup> Dipartimento di Biotecnologie Mediche, Università di Siena, I-53100 Siena, Italy

<sup>c</sup> Université Clermont-Auvergne, CNRS, SIGMA Clermont, Institut de Chimie de Clermont-Ferrand, 63000 Clermont-Ferrand, France

<sup>d</sup> Laboratoire des Macromolécules Biologiques, Centre d'Ingénierie des Protéines-InBioS, Université de Liège, Institute of Chemistry B6a, Sart-Tilman, 4000 Liège, Belgium

<sup>e</sup> Laboratoire de Biochimie, Centre d'Ingénierie des Protéines-InBioS, Université de Liège, Allée du 6 août B6, Sart-Tilman, 4000 Liège, Belgium

<sup>f</sup> Centre d'Ingénierie des Protéines-InBioS, Université de Liège, Allée du 6 août B6, Sart-Tilman, 4000 Liège, Belgium

## ARTICLE INFO

## Keywords:

Metallo- $\beta$ -Lactamase  
1,2,4-triazole-3-thione  
Bacterial resistance  
 $\beta$ -lactam antibiotic

## ABSTRACT

In Gram-negative bacteria, the major mechanism of resistance to  $\beta$ -lactam antibiotics is the production of one or several  $\beta$ -lactamases (BLs), including the highly worrying carbapenemases. Whereas inhibitors of these enzymes were recently marketed, they only target serine-carbapenemases (e.g. KPC-type), and no clinically useful inhibitor is available yet to neutralize the class of metallo- $\beta$ -lactamases (MBLs). We are developing compounds based on the 1,2,4-triazole-3-thione scaffold, which binds to the di-zinc catalytic site of MBLs in an original fashion, and we previously reported its promising potential to yield broad-spectrum inhibitors. However, up to now only moderate antibiotic potentiation could be observed in microbiological assays and further exploration was needed to improve outer membrane penetration. Here, we synthesized and characterized a series of compounds possessing a diversely functionalized alkyl chain at the 4-position of the heterocycle. We found that the presence of a carboxylic group at the extremity of an alkyl chain yielded potent inhibitors of VIM-type enzymes with  $K_i$  values in the  $\mu$ M to sub- $\mu$ M range, and that this alkyl chain had to be longer or equal to a propyl chain. This result confirmed the importance of a carboxylic function on the 4-substituent of 1,2,4-triazole-3-thione heterocycle. As observed in previous series, active compounds also preferentially contained phenyl, 2-hydroxy-5-methoxyphenyl, naphth-2-yl or *m*-biphenyl at position 5. However, none efficiently inhibited NDM-1 or IMP-1. Microbiological study on VIM-2-producing *E. coli* strains and on VIM-1/VIM-4-producing multidrug-resistant *K. pneumoniae* clinical isolates gave promising results, suggesting that the 1,2,4-triazole-3-thione scaffold worth continuing exploration to further improve penetration. Finally, docking experiments were performed to study the binding mode of alkanolic analogues in the active site of VIM-2.

## 1. Introduction

The development and spread of bacteria resistant to antibiotics have become a very serious threat to public health [1]. Because bacterial

resistance reached alarming levels, academics, pharmaceutical industries and governments are urgently implementing a global response to resolve this crisis. In this context, WHO has recently established a “global priority list of antibiotic-resistant bacteria” to fight [2]. The first

**Abbreviations:** BL,  $\beta$ -lactamase; Boc, *tert*-butoxycarbonyl; CFU, colony forming unit; DCM, dichloromethane; DIEA, diethylisopropylamine; DMF, dimethylformamide; DMSO, dimethylsulfoxide; DPT, dipyridylthionocarbonate; EDTA, Ethylene diamine tetraacetic acid; EtOAc, ethyl acetate; EUCAST, European Committee on Antimicrobial Susceptibility Testing; HEPES, 4-(2-Hydroxyethyl)-1-piperazine-ethanesulfonic acid; HPLC, high performance liquid chromatography; IMP, imipenemase; ITC, isothermal calorimetry; KPC, *Klebsiella pneumoniae* carbapenemase; LC-MS, liquid chromatography coupled to mass spectrometry; MBL, metallo- $\beta$ -lactamase; MEM, Meropenem; MHB, Mueller-Hinton broth; MIC, Minimum Inhibitory Concentration; NDM, New Delhi MBL; OXA, oxacillinase; T3P, propylphosphonic anhydride; TFA, trifluoroacetic acid; VIM, Verona Integron encoded MBL.

\* Corresponding authors.

E-mail addresses: [laurent.gavara@umontpellier.fr](mailto:laurent.gavara@umontpellier.fr) (L. Gavara), [jddocquier@unisi.it](mailto:jddocquier@unisi.it) (J.-D. Docquier), [jean-francois.hernandez@umontpellier.fr](mailto:jean-francois.hernandez@umontpellier.fr) (J.-F. Hernandez).

<https://doi.org/10.1016/j.bioorg.2021.105024>

Received 4 March 2021; Received in revised form 19 May 2021; Accepted 22 May 2021

Available online 26 May 2021

0045-2068/© 2021 Elsevier Inc. All rights reserved.

and critical priority concerns multi- to extremely-drug resistant Gram-negative opportunistic pathogens (i.e. *Acinetobacter baumannii*, *Pseudomonas aeruginosa* and *Enterobacteriaceae* like *Klebsiella pneumoniae* and *Escherichia coli*), which are resistant to carbapenems, considered last resort antibiotics in the hospital, and to late-generation cephalosporins. These drugs belong to the family of  $\beta$ -lactam antibiotics, the most widely used group of antibacterial agents.

The most relevant resistance mechanism to  $\beta$ -lactam antibiotics is the production of enzymes called  $\beta$ -lactamases, which inactivate them via hydrolysis of their  $\beta$ -lactam ring [3–6].  $\beta$ -Lactamases are divided into classes A, B, C, and D [7], according to their primary and tertiary structures, and their catalytic mechanism. Classes A, C and D are serine hydrolases, which show a heterogeneous substrate profile, mainly concerning penicillins and cephalosporins. But few of them (e.g. the class A KPC- and the class D OXA-48-type enzymes) also inactivate carbapenems. By contrast, class B enzymes, called metallo- $\beta$ -lactamases (MBLs) because they use one or two Zn atom(s) for catalysis, are all efficient carbapenemases, often characterized by a broad substrate profile, including penicillins and cephalosporins. MBLs are subdivided into subclasses B1, B2, and B3, based on structural features [8]. Among these, the most clinically relevant enzymes are di-zinc MBLs belonging to subclass B1 (e.g. VIM-, NDM-, and IMP-types). MBLs are produced by those Gram-negative bacteria belonging to the WHO first priority list, which are responsible of life-threatening nosocomial infections. In addition, although initially spreading in the hospital setting, MBL-producing isolates are now increasingly causing community-acquired infections [9]. Due to the global dissemination of MBL-producing isolates, these enzymes are major therapeutic targets [10].

Inhibiting  $\beta$ -lactamases to protect  $\beta$ -lactam drugs is a well-known approach and several  $\beta$ -lactamase inhibitors are currently marketed (e.g. clavulanate, tazobactam, avibactam, vaborbactam) [11]. However, they only target some serine- $\beta$ -lactamases (SBLs) [12]. Two MBL inhibitors are under clinical development (phase III trials for taniboractam, phase I for QPX7728) [13–16], and only few other compounds are promising [17–19]. In fact, one major difficulty is the existence of numerous MBLs showing subtle differences in their active sites and the discovery of a broad-spectrum inhibitor is a true challenge [12,20,21]. In addition, most inhibitors typically possess a zinc-coordinating group, therefore presenting a potential risk to inhibit important human metallo-enzymes [22].

Among numerous reported families of MBL inhibitors, the largest one possesses a thiol group [e.g. [23–25]], which was also largely used to inhibit human metallo-peptidases (e.g. captopril). The consequence is a high risk for insufficient selectivity. Another important family contains compounds with at least two carboxylate groups, another well-known Zn-ligand, such as succinate [26] or dipicolinate [27] analogues, or as aspergillomarasmine [28], whose inhibition mechanism at least partially involves zinc removal [29]. Insufficient selectivity is also a potential limitation for these compounds [30]. Another Zn-chelating MBL inhibitor, Zn148, was also recently reported [31]. Finally, bicyclic boronates, such as taniboractam and QPX7728, are currently the most promising candidates [14,15,32,33], being inhibitors of both MBLs and SBLs.

In this context, we are developing MBL inhibitors using the 1,2,4-triazole-3-thione scaffold as an original and promising ligand for the di-zinc active sites of these enzymes [34,35]. Otto Dideberg's group previously identified the binding mode of the 4-amino-5-substituted analogue IIIA (Fig. 1) in the di-zinc subclass B3 MBL L1 [36]. The compound simultaneously bound to the two Zn ions through two atoms of its heterocyclic moiety ( $N^2$  for Zn1 and  $S^3$  for Zn2). A similar binding was more recently established for the di-zinc subclass B1 MBLs VIM-2 [37,38] and NDM-1 [39]. It is also noticeable that several other studies, including random in silico and experimental screenings, identified this heterocycle as a potential scaffold for the inhibition of IMP-1 [40], VIM-2 [37] and NDM-1 [41]. Compared to other zinc-binding groups, the specific behaviour of the 1,2,4-triazole-3-thione moiety should favour selectivity toward human metallo-enzymes, which are mainly mono-zinc.

After Dideberg's study [36], we launched an extensive exploration of the 1,2,4-triazole-3-thione scaffold. We first reported a series of IIIA-based analogues (Fig. 1), diversely substituted at position 5 and substituted or not at position 4 by a  $NH_2$  group [42]. Activities were generally modest, but few compounds displayed micromolar and broad-spectrum inhibition against a panel of representative MBLs, including VIM-2, NDM-1 and IMP-1. However, no compound showed activity in microbiological assays. This structure–activity relationship study yielded valuable information about the most favourable substituents at position 5. These results were confirmed with a series of Schiff base analogues diversely substituted at positions 4 and 5 (Fig. 1) [38]. In addition, the presence of an aryl substituent at position 4 linked to the heterocycle by a hydrazone-like bond led to the discovery of more potent compounds with a broad spectrum of inhibition. In particular, several favourable aryl groups including an *o*-benzoic group were identified. Another series of molecules possessing a hydrazine-like bond (i.e. corresponding to the reduced form of Schiff base analogues, Fig. 1) yielded similar inhibitory activities although of lower impact [43]. However, again, only limited antibiotic potentiation was obtained in microbiological assays. These results were mainly explained by a poor bacteria outer membrane penetration. To try to solve this issue, we continued to explore other types of substituents at position 4 of the triazole ring and undertook the synthesis of analogues where the hydrazone- or hydrazine-like function was replaced by alkyl linkers.

We herein report on a new series of 1,2,4-triazole-3-thione compounds where the position 4 was substituted by diversely functionalized alkyl chains (Fig. 1). The main results were the restriction of the inhibition spectrum to VIM-type enzymes compared to previous series of analogues but with compounds showing promising activity in microbiological assays, including against MBL-producing clinical isolates.

## 2. Results and discussion

### 2.1. Synthesis

All compounds were prepared according to [44]. The hydrazide precursor of substituent at position 5 was first obtained in two steps from

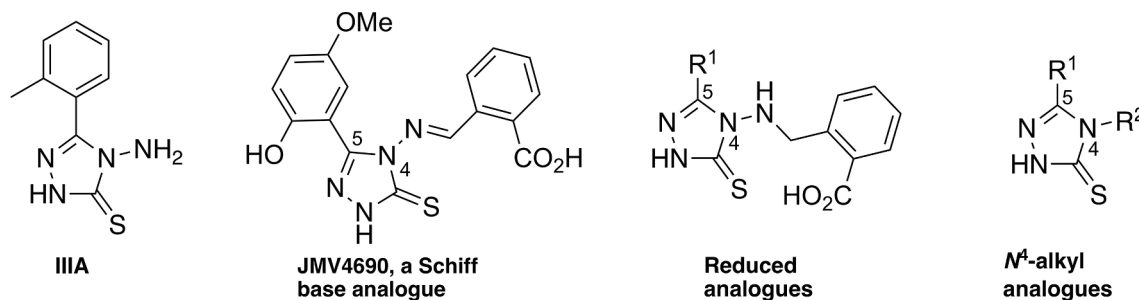


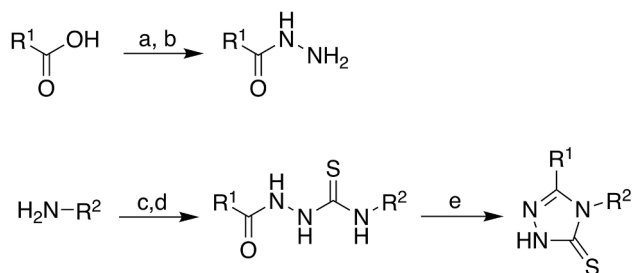
**Fig. 1.** Structure of compound IIIA [36,42], JMV4690, a representative Schiff base analogue [38], the reduced analogues [43] and synthesized 4-alkyl analogues ( $R^1$  = (hereto)aryl-( $CH_2$ )<sub>n</sub>- with  $n = 0-2$ ;  $R^2$  = alkyl functionalized or not).

the corresponding carboxylic acid. Then, the alkylamines  $R^2-NH_2$ , either commercially available or prepared as described in [Supporting Information](#), were treated with DPT (dipyridylthionocarbonate) to yield the intermediate isothiocyanates, which were directly reacted with hydrazides to form the thiosemicarbazide derivatives. Their basic treatment yielded the expected 1,2,4-triazole-3-thione compounds. Specific synthetic steps carried out for the preparation of several compounds are presented in [Scheme 2](#). The hydroxamate **4** was prepared by coupling **3** to O-trityl-hydroxylamine, followed by trityl removal in acidic conditions. Compound **8** was obtained from the Boc-protected precursor and was reacted with: (i) benzoyl chloride and *p*-tosyl-chloride to yield compounds **9** and **12**, respectively; (ii) DPT as described in [Scheme 1](#), followed by condensation with benzhydrazide and hot basic treatment to give the di-triazole-thione compound **15**; (iii) phthalic anhydride in refluxing pyridine to yield the phthalimide **10**, which was opened in basic conditions to afford **11**. Compound **38** was obtained from **39** through Boc removal (the same was performed for **36** from **37**) and was condensed to phenylisocyanate to yield the urea **40**.

## 2.2. Evaluation of inhibitory potency toward purified MBLs

Compounds were tested against five representative MBLs, the subclass B1 enzymes VIM-2, VIM-4, NDM-1 and IMP-1, and the subclass B3 L1. Few compounds were also tested against VIM-1. Initially, testing was performed at one concentration (100 or 200  $\mu$ M) and  $K_i$  values were measured for compounds showing significant inhibition (typically > 75%). As all compounds evaluated against L1 were no or low inhibitors (<50% inhibition at 100  $\mu$ M) of this enzyme, we chose to not include these results in the Tables.

The results obtained for a first series of 19 compounds are presented in [Table 1](#). In this series, all compounds possessed a phenyl ring at position 5 and differed by the alkyl substituent at position 4, itself possibly carrying additional substituents. Two compounds (**1** and **2**) contained a non-functionalized saturated alkyl chain, while others displayed diverse functional groups such as carboxyl (**3**), hydroxamate (**4**), alcohol (**5**, **6**), sulfonic (**7**), amine (**8**, **14**), amide (**9–11**, **16**), sulphonamide (**12**), urea (**13**), azide (**17**), sulfonyl (**18**) and unsaturated alkyl chain (**19**). In particular, compounds **9–14** were derivatives of the amine **8**. Finally, compound **15** can be considered as a dimeric 5-phenyl-1,2,4-triazole-3-thione where the two monomers were linked by an ethylene group at their 4-position. Overall, most compounds showed poor or no inhibition towards any MBL tested. In particular, NDM-1 and IMP-1 were not significantly inhibited by any compound with the exception of compound **1**, which showed a  $K_i$  of around 30  $\mu$ M against IMP-1. To note, a close analogue of the NDM-1-inactive compound **19** differing by the presence of a 2-hydroxyphenyl ring at position 5 has been previously reported in the literature as a potent NDM-1 inhibitor [\[41\]](#). In our hands, however, this compound was also found inactive against NDM-1 (<20% inhibition at 100  $\mu$ M), supporting the fact that the allyl group was not more favourable to NDM-1 inhibition than other substituents placed at position 4 in this series.



**Scheme 1.** Synthesis of 4-alkyl-1,2,4-triazole-3-thione derivatives. *Reagents and conditions:* (a) EtOH,  $H_2SO_4$ , reflux, 5 h; (b) EtOH, hydrazine hydrate, 100 °C, sealed tube; (c) DPT, DMF, sealed tube, 55 °C, 3 h; (d)  $R^1-CONHNH_2$ , DMF, 55 °C, 3 h; (e) aqueous KOH or  $NaHCO_3$ , 100 °C, 3 h.

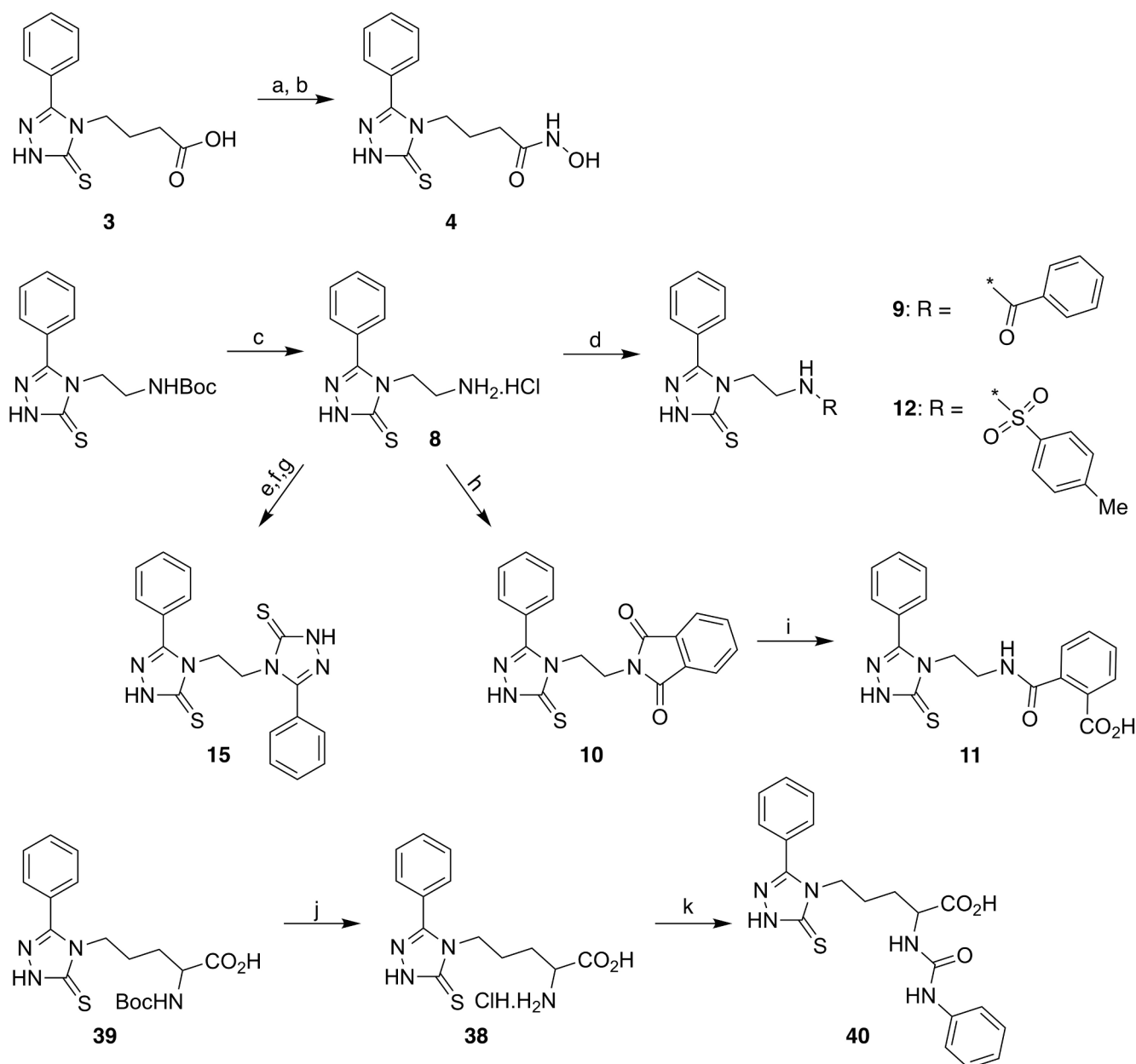
Overall, five compounds displayed  $K_i$  values in the micromolar to submicromolar range against both VIM-2 and VIM-4. Compounds **1** and **2** had a non-functionalized linear butyl and hexyl chain, respectively, while compounds **3**, **5** and **16** contained a butanoic, a butanol or a pyrrolidinone moiety, respectively. Few other compounds showed more modest activities ( $K_i$  values in the 10–40  $\mu$ M range) against VIM-2 and/or VIM-4 (i.e. **4**, **6**, **10**, **11**, **13**, **14**, **15**, **17–19**) with often a preference for VIM-4. Finally, in this first series, four compounds, **3**, **5**, **6** and **19**, were tested against VIM-1 and showed modest to good inhibitory potencies ( $K_i$ 's,  $39.8 \pm 6.7$   $\mu$ M,  $1.69 \pm 0.12$   $\mu$ M,  $6.15 \pm 0.33$   $\mu$ M,  $4.25 \pm 0.32$   $\mu$ M, respectively).

According to these first results and as the presence of a carboxylic group on the substituent at position 4 has already been highlighted in previous series [\[38,43\]](#), we kept it in a second group of 20 compounds bearing various alkanolic moieties and a phenyl ring at the 5-position ([Table 2](#), compound **3** was added for comparison). We varied the length of the alkanolic chain (**20**, **22**, **23**, **26**, **27**), introduced an amide bond (**21**), heteroatoms (O for **24**, S for **25**), aromatic rings (**28–31**), cyclohexyl moieties (**32–34**), or an amine group, protected (**36**, **38**, **39**) or not (**35**, **37**). As in the case of the first series, all compounds were inactive or only moderately active against NDM-1 and IMP-1: the best compounds against NDM-1 displayed longer alkanolic chains (i.e. hexanoic for **26** and octanoic for **27**) and showed  $K_i$  values in the 15–20  $\mu$ M range. In this series, VIM-2 and VIM-4 inhibition could be retained or slightly improved. For these enzymes, the alkyl length was important as compounds with an alkanolic chain shorter than butanoic (acetic **20**, propionic **22**) were poorly or not active, whereas those with longer ones (pentanoic **23**, hexanoic **26** and octanoic **27**) showed similar or higher (i.e. submicromolar range) inhibitory potencies compared to compound **3**. Compound **27** displayed the best  $K_i$  values (0.33 and 0.49  $\mu$ M, respectively) against VIM-2 and VIM-4 in this series. In addition, although compound **23** was moderately active against VIM-1 as compound **3**, compounds **26** and **27** with a longer alkanolic chain were micromolar inhibitors of this enzyme. Introducing a sulfur but not an oxygen in the alkyl chain of compound **23** was favourable for both VIM-type enzymes. Indeed, whereas the ether analogue **24** was moderately or not active against VIM-2 and VIM-4, respectively, the thioether **25** displayed micromolar to submicromolar  $K_i$  values against the same enzymes. In addition, this compound was also a micromolar inhibitor of VIM-1 and moderately inhibited NDM-1, indicating that the sulfur atom significantly improved MBL inhibition.

Branching a phenyl ring at the  $\beta$  position of the butanoic chain of **3** yielded compounds **28** and **29**, which were slightly better inhibitors of VIM-1, VIM-2 and VIM-4 compared to **3**. Constraining the alkanolic chain with a cyclohexyl moiety as in **32–34** was well tolerated for VIM-2 and VIM-4 inhibition. However, compared to the closest analogues **3** and **26**, no improvement was observed, with the exception of **34** which was a better VIM-1 inhibitor.

As a carboxylate group could be unfavourable for external membrane penetration, the adjunction of a protonated or protonatable nitrogen atom in a molecule is a frequent mean to counteract the effect of a negative charge, leading to a zwitterionic form expected to more favourably penetrate through porins [\[45\]](#). Unfortunately, replacing the phenyl ring of compound **28** by a pyridine (i.e. **30** and **31**) was detrimental. Also, introducing an amine group at the  $\alpha$  position of the butanoic chain (i.e. **35**) abolished VIM-2 inhibition, and the addition of a Boc group was not favourable either (i.e. **36**). The same was true for the  $\alpha$ -amino analogue of compound **23** (i.e. **37**). However, in contrast, its Boc-protected derivative **38** showed similar activities to **23** against VIM-2 and VIM-4 with  $K_i$  values in the low micromolar range, suggesting that the presence of a hydrophobic and bulky group was suitable at this position. This was confirmed when attaching a phenyl ring to the amine via a urea link. Although less potent, the corresponding compound **39** significantly inhibited VIM-type enzymes.

Overall, the presence of a hydrophobic linear or constrained alkyl chain at position 4 was favourable to inhibition of VIM-type enzymes as compounds **3**, **23**, **25**, **26**, **27** and **32–34** were potent inhibitors of these



**Scheme 2.** Specific steps for the synthesis of compounds **3**, **4**, **8–12**, **15**, **38–40**. Reagents and conditions: (a) *O*-trityl-hydroxylamine, T3P, DIEA, DMF; (b) TFA, DCM, triisopropylsilane; (c) 15% conc. HCl in dioxane, anisole; (d) Cl-R, DIEA, DMF; (e) DPT, DMF, sealed tube, 55 °C, 3 h; (f) benzhydrazide, DMF, 55 °C, 3 h; (g) aqueous KOH, EtOH, 100 °C, 3 h; (h) phthalic anhydride, pyridine, reflux; (i) KOH (10 equiv.), EtOH, water, rt; (j) 15% conc. HCl in dioxane, anisole; (k) phenylisocyanate, DIEA, EtOH, dioxane.

MBLs with  $K_i$  values in the micromolar range, and even submicromolar in the case of compounds **25–27**. Branching a phenyl ring (**28**, **29**) or a blocked amine group (**38**, **39**) was also compatible with inhibition of the same enzymes.

To try to get more insight in the structure–activity relationships in this series, we selected some compounds and calculated the theoretical pKa values of their carboxylic group using the pKa module of MarvinSketch software (see Table S1). We also calculated the ligand efficiencies (LE, Table S1) toward VIM-2 as a representative VIM-type enzyme. However, no clear correlation could be drawn between pKa values and the inhibitory potencies, even for compounds having a carboxylic group at the same distance from the triazole ring (i.e. **21**, **23–25**, **37–39**). As stated above, other features like the alkyl chain length or the presence of hydrophobic and/or bulky moieties are determining.

Based on these results, we prepared a third series of 28 compounds possessing either a butanoic or a pentanoic chain at position 4 and a

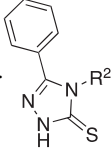
variable substituent at position 5 (Table 3). Parent compounds **3** (4-butanoic) and **23** (4-pentanoic) were included for comparison.

Most substituents here introduced at position 5 were explored in preceding series [38,42,43]. It included *o*-toluyl (**40**, **41**), halogenated phenyls (**42–44**), methoxy-phenyls (**45–47**), heteroaryls (**48–54**, **57–59**, **62**, **66**), biaryls (**55–61**, **63**, **65**, **66**), phenethyl (**64**) and cyclohexyl (**67**). Some of these were previously shown favourable to broad-spectrum inhibition, as halogenated aryls, 2-hydroxy-5-methoxy-phenyl, naphthyls, *m/p*-biphenyls and *p*-benzyloxyphenyl.

Unfortunately, as compounds **3** and **23**, all compounds were inactive or only moderately active ( $K_i$  of around 100  $\mu$ M for compound **60** against NDM-1) against NDM-1 and IMP-1. Several compounds (**40–47**, **50–53**, **55–58**, **60**, **61**) significantly inhibited VIM-2 and/or VIM-4 with  $K_i$  values in the micromolar to submicromolar range. All 5-substituents of these compounds were aryl or heteroaryl groups directly attached to the triazole ring. Finally, when the comparison was possible (**3/23**, **40/**

**Table 1**Inhibitory activity of 4-alkyl-1,2,4-triazole-3-thiones **1–19** with R<sup>1</sup> = phenyl

against various MBLs.



Cpd	Structure R <sup>2</sup>	K <sub>i</sub> (μM) or (% inhibition at 100 μM)			
		VIM-2	VIM-4	NDM-1	IMP-1
<b>1</b>		2.43 ± 0.21	1.20 ± 0.13	NI	31.8 ± 3.9
<b>2</b>		4.94 ± 0.19	0.31 ± 0.03	NI	NI
<b>3</b>		7.23 ± 0.68	1.47 ± 0.20	NI	NI
<b>4</b>		16.1 ± 2.4	10.6 ± 1.6	NI	NI
<b>5</b>		6.17 ± 0.55	3.86 ± 0.19	NI	NI
<b>6</b>		40.2 ± 13.8	11.4 ± 1.7	NI	NI
<b>7</b>		NI	- <sup>a</sup>	NI	NI
<b>8</b>		NI	NI	NI	NI
<b>9</b>		NI	NI	NI	NI
<b>10</b>		11.4 ± 1.2	NI	NI	NI
<b>11</b>		18.4 ± 3.6	12.3 ± 1.1	NI	NI
<b>12</b>		NI	NI	(35%)	NI
<b>13</b>		17.9 ± 6.1	10.4 ± 1.2	NI	NI
<b>14</b>		13.7 ± 2.9	7.8 ± 1.3	NI	NI
<b>15</b>		11.7 ± 1.4	4.1 ± 0.6	NI	NI
<b>16</b>		5.32 ± 0.76	2.60 ± 0.18	NI	NI
<b>17</b>		27.7 ± 5.4	NI	NI	(31%)

**Table 1 (continued)**

Cpd	Structure R <sup>2</sup>	K <sub>i</sub> (μM) or (% inhibition at 100 μM)			
		VIM-2	VIM-4	NDM-1	IMP-1
<b>18</b>		13.4 ± 2.2	5.70 ± 0.58	NI	NI
<b>19</b>		17.8 ± 4.4	8.8 ± 0.8	NI	(45%)

NI: No Inhibition (&lt;30% or &lt; 50% inhibition at 100 or 200 μM, respectively).

<sup>a</sup>Not determined. All kinetic assays were performed in triplicate.

**41, 46/47, 55/56**), no significant difference could be observed between butanoic and pentanoic compounds. Overall, compound **60** displayed the best activities against VIM-1, VIM-2 and VIM-4 in this series with K<sub>i</sub> values of 5.50, 0.35 and 0.27 μM, respectively, confirming the interest of a *m*-biphenyl at position 5 [38,42,43].

### 2.3. Isothermal calorimetry experiments (ITC)

To validate the binding mode of compounds to VIM-2, isothermal titration calorimetry was performed with compound **3**. The thermodynamic parameters of binding are given in Table 4 and are also depicted in Fig. 2A for a more visual inspection. An ITC thermogram is shown in Fig. 2B.

The experiment showed a stoichiometric relationship between VIM and 2 and the inhibitor, which clearly indicated a 1:1 association. Compound **3** binding was enthalpy-driven (the enthalpic term is the major contributor to ΔG°<sub>b</sub> and therefore to affinity). The favorable enthalpy contribution is an indication of specific interactions between binding partners and reflects ligand specificity and selectivity. Compound **3** also displayed a favorable entropic contribution, which is regarded as resulting from the release of organized water molecules at the surface of individual partners to the bulk solvents. Overall, this suggests that favorable enthalpic interactions, mainly electrostatic, occurring in the complex were replacing pre-existing bonds established with the solvent water [46,47]. Accordingly, the net enthalpic effect is reduced due to desolvation and, as a result, the affinity remained moderate. The K<sub>d</sub> value was in the same range as the K<sub>i</sub> value.

### 2.4. In vitro antibacterial synergistic activity and cytotoxicity

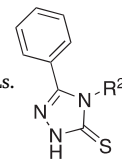
The ability of selected compounds to potentiate the activity of β-lactam antibiotics was first evaluated using a disk diffusion assay performed on isogenic MBL-producing laboratory *Escherichia coli* strains, obtained by transforming strain AS19 (a chemically mutagenized strain with enhanced permeability) or LZ2310 (a triple knock-out mutant of K12 in which genes encoding components of the major efflux pumps NorE, MdfA and AcrA were inactivated) with a derivative of the pLB-II plasmid in which the bla<sub>VIM-2</sub> gene was cloned [48]. The latter strain was used to limit the potential efflux of the compounds, which would prevent sufficient accumulation in the periplasm. Compounds were tested according to their inhibition profile (Table 5).

In this assay, the two potent VIM-2 inhibitors **3** and **23** significantly potentiated the activity of cefoxitin on the VIM-2-producing LZ2310 strain (Table 5, Figure S1). Indeed, they restored susceptibility to the antibiotic (being above the EUCAST resistance breakpoint, 18 mm), as a diameter of the growth inhibition zone of 19–20 mm was measured. However, a more limited effect was observed when these compounds were tested on the AS19 strain, potentially indicating the role of efflux pumps in preventing a significant accumulation of the compounds in the periplasm. Nonetheless, compound **23** also provided some detectable potentiation of cefoxitin on VIM-2-producing AS19 strain. Both compounds **3** and **23** possess a phenyl ring at position 5 and only differ by one CH<sub>2</sub> in the alkyl chain at position 4, which could explain their



Table 2

Inhibitory activity of 4-alkyl-1,2,4-triazole-3-thiones **3**, **20–39** with R<sup>1</sup> = phenyl and R<sup>2</sup> containing a carboxylic function against various MBLs.



Cpd	Structure	K <sub>i</sub> (μM) or (% inhibition at <sup>a</sup> 100 or <sup>b</sup> 200 μM)				
	R <sup>2</sup>	VIM-1	VIM-2	VIM-4	NDM-1	IMP-1
<b>3</b>		39.8 ± 6.7	7.23 ± 0.68	1.47 ± 0.20	NI	NI
<b>20</b>		- <sup>c</sup>	44.3 ± 0.2	(40%) <sup>a</sup>	NI	NI
<b>21</b>		NI	9.54 ± 1.21	6.79 ± 0.60	NI	NI
<b>22</b>		–	NI	(30%) <sup>a</sup>	NI	NI
<b>23</b>		13.9 ± 1.1	2.81 ± 0.58	1.13 ± 0.12	NI	(60%) <sup>b</sup>
<b>24</b>		–	14.3 ± 2.0	NI	NI	NI
<b>25</b>		2.36 ± 0.14	0.81 ± 0.04	0.71 ± 0.06	(40%) <sup>a</sup>	NI
<b>26</b>		5.05 ± 0.26	0.72 ± 0.10	1.36 ± 0.10	19.7 ± 0.2	NI
<b>27</b>		1.27 ± 0.08	0.33 ± 0.02	0.49 ± 0.02	15.7 ± 1.8	(40%) <sup>a</sup>
<b>28</b>		18.5 ± 1.3	0.80 ± 0.04	1.04 ± 0.26	NI	NI
<b>29</b>		24.3 ± 2.1	1.32 ± 0.17	0.42 ± 0.02	NI	NI
<b>30</b>		–	NI	NI	NI	NI
<b>31</b>		NI	NI	NI	NI	NI
<b>32</b>		–	8.06 ± 0.94	6.54 ± 0.25	NI	NI
<b>33</b>		–	6.54 ± 0.64	3.08 ± 0.23	NI	NI
<b>34</b>		2.82 ± 0.34	2.87 ± 0.22	0.85 ± 0.08	NI	NI
<b>35</b>		–	NI	–	NI	NI
<b>36</b>		–	NI	–	NI	NI

(continued on next page)

Table 2 (continued)

Cpd	Structure	$K_i$ ( $\mu$ M) or (% inhibition at <sup>a</sup> 100 or <sup>b</sup> 200 $\mu$ M)				
	R <sup>2</sup>	VIM-1	VIM-2	VIM-4	NDM-1	IMP-1
37		–	NI	NI	NI	NI
38		–	1.95 $\pm$ 0.11	1.51 $\pm$ 0.08	NI	NI
39		(57%) <sup>a</sup>	6.93 $\pm$ 1.08	4.14 $\pm$ 0.39	(30%) <sup>a</sup>	NI

NI: No Inhibition (<30% or < 50% inhibition at 100 or 200  $\mu$ M, respectively). <sup>a</sup>% inhibition at 100  $\mu$ M; <sup>b</sup>% inhibition at 200  $\mu$ M; <sup>c</sup>Not determined. All kinetic assays were performed in triplicate.

similar *in vitro* activity.

Other compounds, despite being similarly potent VIM-2 inhibitors (i.e. compounds **16**, **32**, **40**, **46** and **55**), did not show any antibiotic potentiation, indicating that they might not be able to efficiently cross the outer membrane and accumulate in the periplasm at biologically relevant concentrations. In particular, compounds **40**, **46** and **55** are analogues of compound **3** differing by their substituent at position 5 (respectively, *o*-toluyl, 2-hydroxy-5-methoxy-phenyl and 2-naphthyl). A similar influence of this substituent was already observed in the Schiff base series (Fig. 1), as only the analogue with an unsubstituted phenyl ring at position 5 was found active in the same assay [38].

We also tested the ability of some compounds to increase the meropenem susceptibility of MBL-producing multidrug-resistant clinical isolates using a broth microdilution method. As the most potent inhibitors of the present series are mainly targeting VIM-type enzymes, we chose two *K. pneumoniae* isolates producing VIM-1 and VIM-4. Compounds were tested at a fixed concentration of 32  $\mu$ g/ml and a low micromolar or submicromolar VIM inhibitory activity was necessary to observe a significant reduction of meropenem MIC on *K. pneumoniae* bacteria (Table 6). In the case of VIM-1-producing bacteria, although not all inhibitory potencies have been determined, several among the most potent VIM-1 inhibitors (i.e. **5**, **6**, **19**, **25**, **27** and **60**) decreased the antibiotic MIC by eight-fold. Less potent inhibitors (i.e. **3**, **23** and **29**) also showed lower potentiating activity. When tested with a VIM-4-producing strain, several compounds showed a 4- to 16-fold potentiation of meropenem. In particular, compound **60**, which was the best VIM-4 inhibitor in this series, also displayed the highest potentiation effect (16-fold) with this isolate. To note, several compounds with similar VIM-4 inhibitory potencies in the low micromolar to submicromolar range (i.e. **1**, **3**, **23**, **25–27**, **29**, **34**, **38**, **47**, **51**, **56**, **60**) showed different levels of MIC reduction (from zero-fold for **47** and two-fold for **23** to eight-fold for **3**, **26** and **34**). These results indicate that subtle structural changes could have significant effects on outer membrane penetration and rate of accumulation in the periplasm. None of the tested compounds showed intrinsic antibacterial activity when tested alone (MIC > 128  $\mu$ g/mL).

These compounds were also evaluated with an NDM-1-producing *E. coli* clinical isolate but none showed any detectable meropenem potentiation (not shown), as expected in consideration of their very low inhibitory activity on this enzyme.

Encouraged by these data, we evaluated whether conditions liable to increase the compound concentration in the bacterial periplasm could further increase their synergistic activity. In particular, compound **60** was tested in the presence of the dipeptide Phe-Arg- $\beta$ -naphthylamide (PA $\beta$ N, 25 and 100  $\mu$ g/mL), a known efflux pump inhibitor [49].

Unfortunately, this combination did not further decrease the MIC of meropenem toward the VIM-1-producing clinical isolate (not shown). Nonetheless, the addition of a subinhibitory concentration (0.12  $\mu$ g/ml) of colistin to the medium did dramatically improve the potentiation activity of **47** (by itself very limited), among the best VIM-4 inhibitors (meropenem MIC, 16 and 2  $\mu$ g/ml in the absence and presence of the inhibitor, respectively; VIM-4-producing *K. pneumoniae* VA-416/02). Furthermore, a similar result was obtained with compound NAB741, a polymyxin derivative without direct antibacterial activity but retaining the outer membrane permeabilizing effect [50,51]. When tested in the presence of 4  $\mu$ g/ml NAB741, meropenem MIC was decreased to 4  $\mu$ g/ml in the presence of the inhibitor. These data overall indicate that the *in vitro* synergistic activity of potent inhibitors are strongly dependent on their ability to rapidly cross the outer membrane barrier and rely on subtle chemical changes in the inhibitor structure.

Furthermore, a preliminary assessment of compound cytotoxicity was carried out using a membrane integrity assay on HeLa cells. Strikingly, no cytotoxic effect could be observed at the highest tested concentration (IC<sub>50</sub> values > 500  $\mu$ M) with compounds **26**, **27** and **60**, selected on the basis of their significant synergistic activity with meropenem on MBL-producing clinical isolates.

Overall, we demonstrated that 1,2,4-triazole-3-thione-based compounds could restore the susceptibility of MBL-producing clinical isolates to a carbapenem, while they do not induce cell lysis of mammalian cells in a cytotoxicity assay, supporting the interest for further medicinal chemistry efforts to improve their membrane permeation properties.

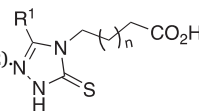
## 2.5. Modelling study

We investigated the putative binding mode of several compounds in the VIM-2 active site with docking experiments. Three compounds containing a butanoic chain at position 4 and a variable substituent at position 5 (**3**, 5-phenyl; **46**, 5-(2-hydroxy-5-methoxy-phenyl); **60**, 5-(*m*-biphenyl)) and a **3** analogue with a hexanoic chain (**26**) were studied.

The docking experiments were performed with a VIM-2 model generated from 6YRP available in the Protein data Bank [38] using AutoDock 4.2. 6YRP is the crystallographic structure of the complex between VIM and 2 and the Schiff base analogue JMV4690 ( $K_i$  = 0.7  $\mu$ M, Figure 1, R1 = 2-hydroxy-5-methoxy-phenyl), which mainly differs from the studied compounds by possessing a rigid hydrazone-like bond and a 2-benzoic acid at position 4 of the triazole ring. (Figure S2). This structure showed the expected double coordination of the active site zinc ions by two atoms of the triazole-thione moiety, and a H-bond network involving the two carboxylate oxygens, the main chain NH of Asn233 and two structural waters (named 5 and 177). In addition, the

Table 3

Inhibitory activity of 4-alkyl-1,2,4-triazole-3-thiones **3**, **23**, **40–67** with  $R^2$  = butanoic ( $n = 1$ ) or pentanoic ( $n = 2$ )



Cpd	Structure		$K_i$ ( $\mu\text{M}$ ) or (% inhibition at <sup>a</sup> 100 or <sup>b</sup> 200 $\mu\text{M}$ )				
	$R^1$	n	VIM-1	VIM-2	VIM-4	NDM-1	IMP-1
<b>3</b>		1	$39.8 \pm 6.7$	$7.23 \pm 0.68$	$1.47 \pm 0.20$	NI	NI
<b>23</b>		2	$13.9 \pm 1.1$	$2.81 \pm 0.58$	$1.13 \pm 0.12$	NI	(60%) <sup>b</sup>
<b>40</b>		1	- <sup>c</sup>	$10.3 \pm 1.1$	$3.13 \pm 0.20$	NI	NI
<b>41</b>		2	-	$3.07 \pm 0.32$	$3.17 \pm 0.22$	NI	NI
<b>42</b>		1	NI	$6.58 \pm 0.48$	$2.10 \pm 0.18$	NI	NI
<b>43</b>		1	-	$8.80 \pm 2.04$	$4.62 \pm 0.32$	NI	NI
<b>44</b>		1	-	$6.39 \pm 0.72$	$4.11 \pm 0.45$	NI	NI
<b>45</b>		1	-	$3.01 \pm 0.19$	$1.70 \pm 0.11$	NI	NI
<b>46</b>		1	NI	$4.20 \pm 0.41$	$1.13 \pm 0.15$	NI	NI
<b>47</b>		2	-	$1.47 \pm 0.14$	$1.31 \pm 0.07$	NI	NI
<b>48</b>		1	-	NI	NI	NI	(65%) <sup>b</sup>
<b>49</b>		1	-	NI	NI	NI	NI
<b>50</b>		1	-	$8.89 \pm 0.58$	$4.84 \pm 0.29$	NI	NI
<b>51</b>		1	-	$6.58 \pm 0.90$	$2.08 \pm 0.09$	NI	NI
<b>52</b>		1	-	$9.27 \pm 1.53$	$4.41 \pm 0.39$	NI	NI
<b>53</b>		1	-	$14.0 \pm 2.2$	$9.09 \pm 1.90$	NI	NI
<b>54</b>		1	-	NI	NI	NI	NI
<b>55</b>		1	NI	$5.56 \pm 0.42$	$0.91 \pm 0.08$	NI	NI
<b>56</b>		2	-	$2.99 \pm 0.32$	$1.56 \pm 0.12$	NI	(60%) <sup>b</sup>
<b>57</b>		1	-	$2.98 \pm 0.29$	$1.91 \pm 0.18$	(50%) <sup>b</sup>	NI
<b>58</b>		1	$30.8 \pm 3.1$	$4.62 \pm 0.32$	$0.31 \pm 0.03$	NI	NI

(continued on next page)



Table 3 (continued)

Cpd	Structure		$K_i$ ( $\mu\text{M}$ ) or (% inhibition at <sup>a</sup> 100 or <sup>b</sup> 200 $\mu\text{M}$ )				
	R <sup>1</sup>	n	VIM-1	VIM-2	VIM-4	NDM-1	IMP-1
59		1	NI	18.2 $\pm$ 2.8	13.3 $\pm$ 4.2	NI	NI
60		1	5.50 $\pm$ 0.67	0.35 $\pm$ 0.14	0.27 $\pm$ 0.13	99.8 $\pm$ 1.6	NI
61		1	NI	3.29 $\pm$ 0.18	1.26 $\pm$ 0.09	NI	NI
62		1	–	NI	NI	NI	NI
63		1	NI	NI	NI	NI	NI
64		1	–	NI	NI	NI	NI
65		1	–	NI	NI	NI	NI
66		1	NI	NI	NI	NI	NI
67		1	–	NI	–	NI	NI

NI: No Inhibition (<30% or < 50% inhibition at 100 or 200  $\mu\text{M}$ , respectively). <sup>a</sup>% inhibition at 100  $\mu\text{M}$ ; <sup>b</sup>% inhibition at 200  $\mu\text{M}$ ; – Not determined. All kinetic assays were performed in triplicate.

Table 4

Thermodynamic parameters of compound **3** binding to VIM-2 at 25 °C.

Cpd	n	$K_a$ ( $\text{M}^{-1}$ )	$K_d$ ( $\mu\text{M}$ )	$\Delta G^\circ_b$ (kcal/mol)	$\Delta H^\circ_b$ (kcal/mol)	$T\Delta S^\circ_b$ (kcal/mol)
3	1.00 $\pm$ 0.01	(6.4 $\pm$ 0.1) $10^5$	1.568	–7.9	–7.0 $\pm$ 0.2	0.9

methoxy group of its 2-hydroxy-5-methoxy-phenyl moiety at position 5 interacted with the indole NH of Trp87.  $\pi$  stacking interactions were also observed between the 5- and 4-aromatic rings and Trp87 and His263, respectively.

First, all studied compounds could be modelled to create similar interactions with the two zinc ions. The triazole nitrogen and sulphur are well positioned to complete the coordination tetrahedron of each zinc. Both compounds possess a carboxylic group at the end of a flexible alkyl chain and no aryl group at the 4-position. Therefore, such compounds lost the advantage of interacting with the His263 side-chain. However, the carboxylic group of compounds with a butanoic substituent (**3**, **46**, **60**) was found to interact as the same group of JMV4690 within the Asn233 pocket (Fig. 3A, B, C). In addition, the Arg228 side-chain seemed to be close enough to complete this interaction network. This is in contrast with the carboxylate group of JMV4690, which was shown to not interact with this basic residue, likely due to the higher rigidity of its carboxylate-bearing cyclic moiety. The docking of compound **26**

provided an interaction similar to that of JMV4690, although the longer alkanolic chain compared to **3** (i.e. hexanoic) did not longer allow the interaction of the carboxylic group within the Asn233 pocket, but ideally placed it to interact with the Arg228 side-chain (Fig. 3D).

Concerning the variable substituent at position 5, the 2-hydroxy-5-methoxy-phenyl moiety of **46** was positioned in a reverse way compared to the same substituent in JMV4690. In this case, the hydroxyl group would establish a H-bond with the side chain of Asp119 (Fig. 3B). The flexibility of the Asp119 side-chain during the docking experiment and the absence of solvent might explain this result as such experiment promotes electrostatic interaction. In the case of compound **60**, the *m*-biphenyl group did not seem to establish particular interactions that could explain its 10-fold higher inhibitory potency compared to the 5-phenyl analogue. An indirect effect could be an increase rigidity because of the bulkier substituent. The hydrophobicity of the biphenyl substituent could displace solvent molecules from the active site, thus contributing a favourable entropic stabilization energy.

The Table S2 presents the mean free energies of best clusters and estimated  $K_i$  values for all four compounds, which were globally consistent with experimental ones.

### 3. Conclusion

By introducing a diversely functionalized alkyl chain at position 4 of 5-substituted 1,2,4-triazole-3-thione derivatives, we found that simple

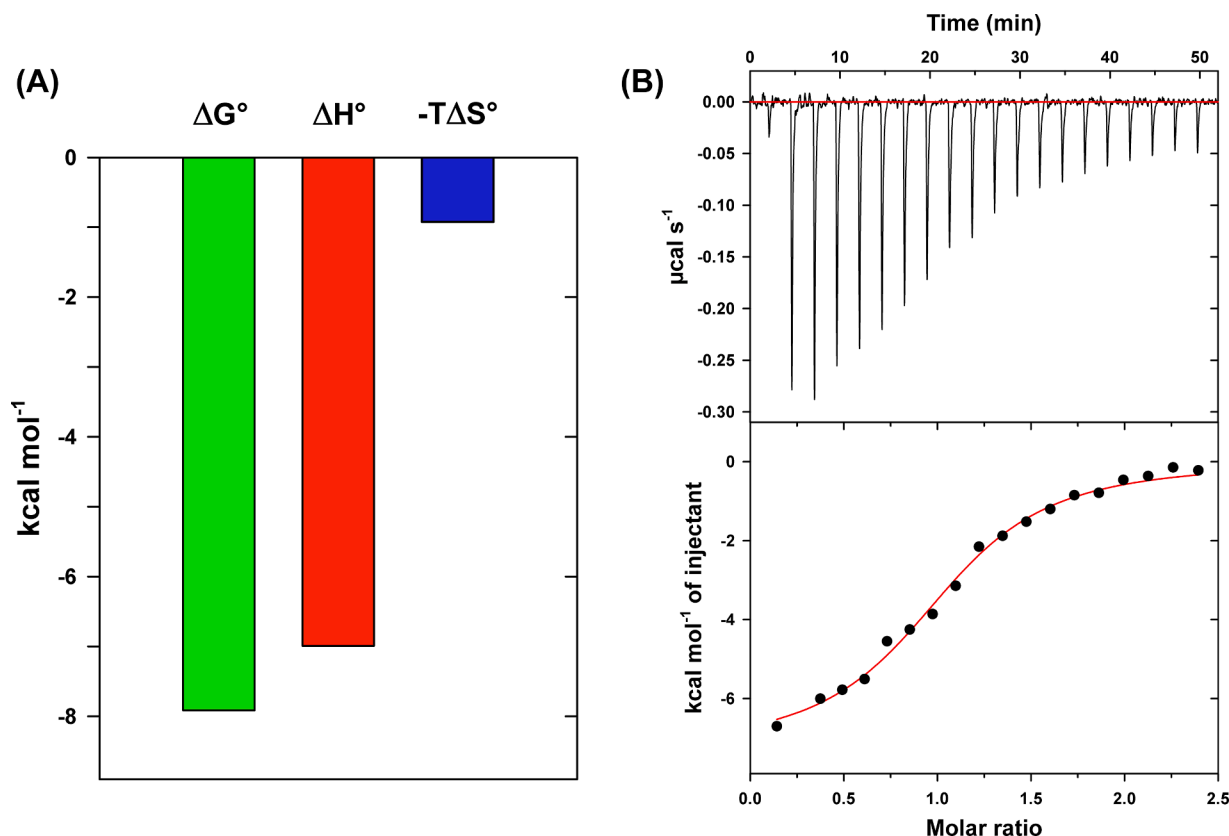


**Fig. 2.** (A) VIM-2 binding energetics of compound 3. Data are from Table 4. (B) Isothermal titration calorimetry of VIM-2 by compound 3 at 25 °C. Upper panel: exothermic microcalorimetric trace of compound injections into VIM-2 solution (18.7 μM). Lower panel: Wiseman plot of heat releases versus molar ratio of injectant/protein in the cell and nonlinear fit of the binding isotherm for  $n$  equivalent binding sites. The binding enthalpy corresponds to the amplitude of the transition curve,  $K_a$  is derived from the slope of the transition and the stoichiometry  $n$  is determined at the transition midpoint.

**Table 5**

In vitro synergistic activity of selected VIM-2 inhibitors measured by disk diffusion assay.<sup>a</sup>

Cpds <sup>b</sup>	$K_i$ (μM) on VIM-2	Inhibition zone diameter (mm) <sup>c</sup>	
		AS19	LZ2310
None	–	16	14
EDTA	–	26	30
DMSO	–	17	14
3	7.23 ± 0.68	ND	20
16	5.32 ± 0.76	17	14
23	2.81 ± 0.58	19	19
32	8.06 ± 0.94	17	15
40	10.3 ± 1.1	17	14
46	4.20 ± 0.41	17	16
55	5.56 ± 0.42	16	14

<sup>a</sup> VIM-2-producing *E. coli* strains were obtained by transforming the pLB-II plasmid carrying the cloned MBL gene in strains AS19 and LZ2310 (triple knock-out mutant of efflux pumps).

<sup>b</sup> A variable volume of the compound dissolved in DMSO was added to a cefoxitin disk (30 μg) in order to obtain a final inhibitor quantity of 40 μg. DMSO was used as a control and did not affect the diameter of the growth inhibition zone. 220 μg EDTA restored full susceptibility to the antibiotic.

<sup>c</sup> EUCAST resistance breakpoint of cefoxitin = 18 mm.

linear alkyl (1, 2), alkanol (5) or alkanolic chains (3, 23, 25–27) were the most favourable for MBL inhibition. In fact, higher potencies were generally measured for compounds with a carboxylic group at the extremity of a linear alkyl chain, the alkyl chain being longer or equal to

**Table 6**

Antibacterial synergistic activity of compounds on VIM-1 and VIM-4-producing *K. pneumoniae* clinical isolates with meropenem (MEM) determined by the broth microdilution method.

Cpd (32 μg/mL)	MEM MIC <sup>a</sup> (μg/mL) and $K_i$ (μM) values of selected inhibitors			
	<i>K. pneumoniae</i> 7023 ( $bla_{VIM-1}$ )		<i>K. pneumoniae</i> VA-416/02 ( $bla_{VIM-4}$ )	
	MEM MIC	$K_i$ (VIM-1) <sup>b</sup>	MEM MIC	$K_i$ (VIM-4) <sup>b</sup>
None	16	–	16	–
1	16	ND	4	1.20 ± 0.13
3	4	39.8 ± 6.7	2	1.47 ± 0.14
4	4	ND	4	10.6 ± 1.6
5	2	1.69 ± 0.12	4	3.86 ± 0.19
6	2	6.15 ± 0.33	8	11.4 ± 1.7
13	8	ND	4	10.4 ± 1.2
19	2	4.25 ± 0.32	4	8.75 ± 0.83
23	8	13.9 ± 1.1	8	1.13 ± 0.12
25	2	2.36 ± 0.14	4	0.71 ± 0.06
26	4	5.05 ± 0.26	2	1.36 ± 0.10
27	2	1.27 ± 0.08	4	0.49 ± 0.02
29	8	24.3 ± 2.01	4	0.42 ± 0.02
33	4	ND	4	3.08 ± 0.23
34	4	ND	2	0.85 ± 0.08
38	8	ND	4	1.51 ± 0.08
47	4	ND	16	1.31 ± 0.07
51	4	ND	4	2.08 ± 0.09
56	8	ND	4	1.56 ± 0.12
60	2	5.50 ± 0.67	1	0.27 ± 0.13

<sup>a</sup> MEM, meropenem.

<sup>b</sup> From Tables 1–3.

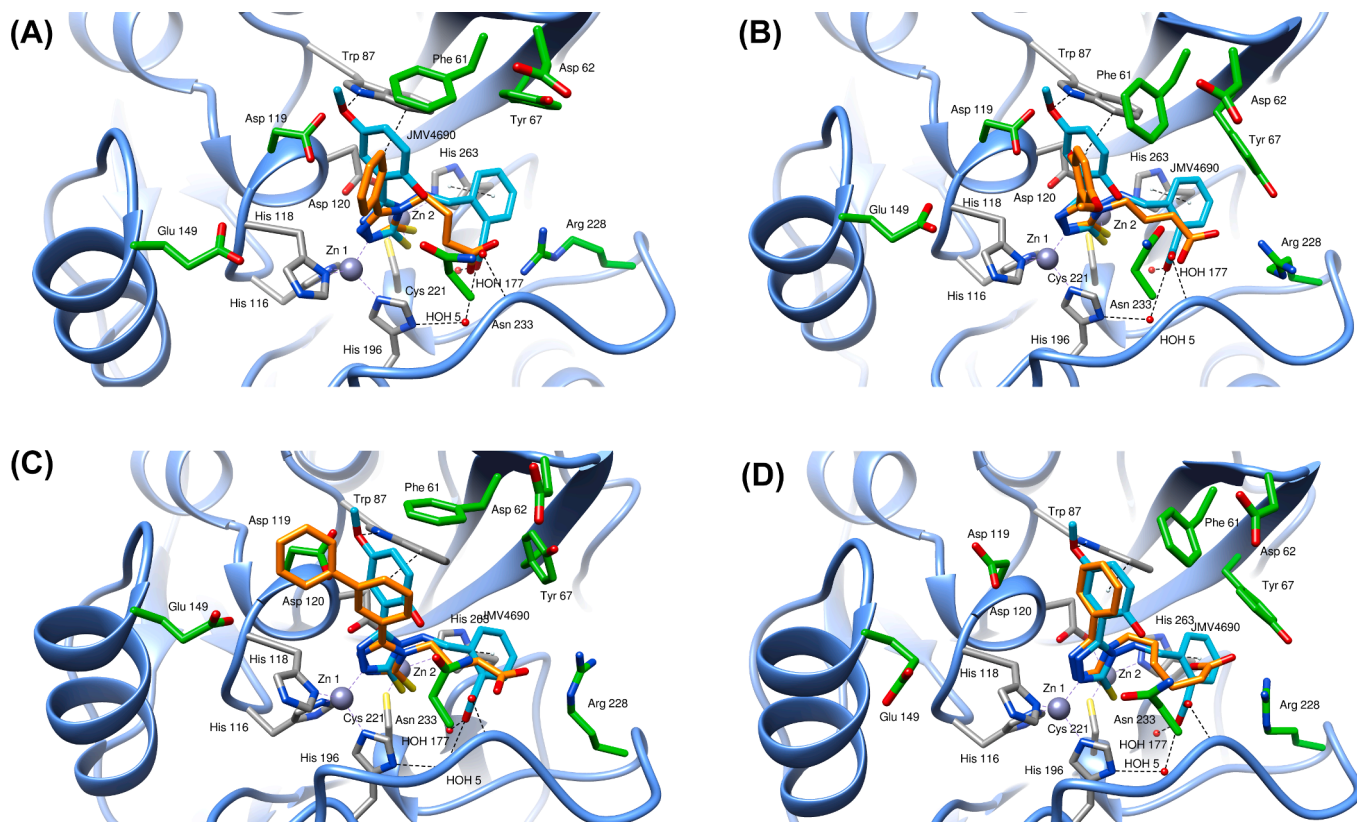


**Fig. 3.** Binding mode of compounds **3** (A), **46** (B), **60** (C) and **26** (D) in VIM-2 studied by molecular modeling. Compounds (orange) were superimposed with JMV4690 (light blue) for comparison. VIM-2 side chains that were let flexible are in green. All four compounds interact with the two zinc ions as determined for JMV4690, while their 5-aryl substituent could present different orientations. The images were produced using UCSF Chimera [52]. (For interpretation of the references to colour in this figure legend, the reader is referred to the web version of this article.)

propyl. A branched substituent like a phenyl ring (**28**, **29**) or a protected amino group (**38**), and a constrained alkyl chain (**32–34**) were also tolerated but without change in potency. VIM-1, VIM-2 and VIM-4 were the only MBLs significantly inhibited among all tested, with  $K_i$  values in the submicromolar to micromolar range. By contrast, NDM-1 and IMP-1 were not or only modestly inhibited by this series of compounds, highlighting a substantial structural heterogeneity between the active sites of these subclass B1 MBLs. As already observed in previous series of 1,2,4-triazole-3-thione compounds, the 4-position is a determining factor for selectivity [38]. Keeping a butanoic or a pentanoic chain at position 4, the study of substitution at position 5 yielded several aryl moieties that were reported favourable in previous series [38,43], i.e. 2-hydroxy-4-methoxy-phenyl (**46**, **47**), naphthyl (**55**, **56**), m-biphenyl (**60**) and benzyloxyphenyl (**61**). Only the m-biphenyl substituent achieved higher VIM-2 and VIM-4 inhibition with  $K_i$  values in the submicromolar range compared to compound **3**, as was observed for the corresponding hydrazone-like [38] and hydrazine-like [43] compounds with an *o*-benzoic group at the 4-position. The modelling study suggested that all docked compounds could interact with the two zinc ions in the VIM-2 active-site as JMV4690 does in the crystallographic structure 6YRP. In addition, the carboxylic group of both compounds with a butanoic chain at position 4, would interact within the Asn233 pocket as the same group of JMV4690. Increasing the alkanic chain length to hexanoic would prevent that interaction but favour ionic interaction with Arg228, therefore allowing to keep similar binding affinity.

Microbiological assays identified two compounds able to potentiate the activity of a  $\beta$ -lactam antibiotic when tested on two VIM-2-producing laboratory strains. More importantly, several compound were found to significantly potentiate the activity of meropenem when tested on two multidrug-resistant VIM-producing *K. pneumoniae* clinical isolates. Compared to previous series [38,43], these inhibitors showed a higher

ability to accumulate in the periplasm at significant concentrations and our data provided some understanding of the structural requirements modulating this aspect.

Despite the compounds displayed a narrower spectrum of MBL inhibition compared to previous series, promising results were obtained in microbiological and cytotoxicity assays, supporting the interest to continue developing this series of 1,2,4-triazole-3-thione-based compounds. Further modification at position 4 of the heterocycle is ongoing to obtain compounds possessing an extended inhibitory spectrum and being able to potentiate the antibiotic susceptibility of MBL-producing clinical isolates. This work will be reported soon.

## 4. Experimental

### 4.1. Chemistry

Hydrazides  $R^1$ -CO-NHNH<sub>2</sub> and non commercial amines  $R^2$ -NH<sub>2</sub> were prepared as described in Supporting Information. Physico-chemical properties of final compounds are also presented in Supporting Information. The purity of final compounds was determined to be  $\geq 95\%$  by <sup>1</sup>H NMR and reverse phase HPLC.

#### 4.1.1. General procedure for the preparation of 4-alkyl-1,2,4-triazole-3-thiones diversely substituted at positions 4 and 5.

Triazole-thione compounds were prepared following the synthetic pathway reported by Deprez-Poulain et al. (2007) [44].

**4.1.1.1. Thiosemicarbazide intermediates.** To a solution of the amine  $R^2$ -NH<sub>2</sub> (1 mmol, 1 equiv.) in anhydrous DMF (4 mL) (in the case of hydrochloride salt, 1.5 equiv. of Na<sub>2</sub>CO<sub>3</sub> (159 mg) was added) was added DPT (244 mg, 1.05 mmol, 1.05 equiv.). After stirring at 55 °C in a

sealed tube for 1 h30, the hydrazide  $R^1$ -CONHNH<sub>2</sub> (1.1 mmol, 1.1 equiv.) was added and the mixture was again heated at 55 °C for 1 h30. After cooling to room temperature, the solution was diluted in EtOAc and the organic phase was extracted five times with water, dried over MgSO<sub>4</sub> and concentrated in vacuum. If necessary, the product was purified by gel column chromatography (EtOAc/Hexane).

**4.1.1.2. Cyclization.** The thiosemicarbazide intermediates were solubilized in a mixture of water and ethanol (2:3) and KOH (3 equiv., 3 mmol) was added. After refluxing for 2 h, the mixture was neutralized with saturated aqueous KHSO<sub>4</sub> and extracted twice with DCM. The organic phases were mixed, dried over MgSO<sub>4</sub>, filtered and evaporated under vacuum. The residues were purified by gel column chromatography (EtOAc/Hexane) or by reverse phase HPLC.

#### 4.1.2. Specific synthetic procedures for compounds **4**, **8–12**, **15**, **35**, **37**, **39**

**4.1.2.1 Compound 4.** A mixture of the carboxylic acid **3** (1 equiv., 0.5 mmol, 135 mg), *O*-trityl-hydroxylamine (1.2 equiv., 0.6 mmol, 165 mg), T3P (1.1 equiv., 0.55 mmol, 175 mg) and DIEA (3 equiv., 1.5 mmol, 0.26 mL) in DMF (4 mL) was stirred at room temperature for 4 h. The solution was then diluted in EtOAc (20 mL) and washed with water (4x30 mL). The organic layer was dried over MgSO<sub>4</sub>, filtered and evaporated. The crude product was purified on silica gel column (EtOAc/Hex) to give the corresponding trityl-protected compound.

A mixture of the trityl-protected intermediate (1 equiv., 0.34 mmol, 177 mg), TFA (10 equiv., 0.25 mL) and triisopropylsilane (11.5 equiv., 0.8 mL) in dichloromethane (8 mL) was stirred at room temperature for 10 min. The residue obtained upon evaporation was purified on silica gel column (DCM/MeOH) to give the corresponding hydroxamic acid **4**.

**4.1.2.1. Compounds 8, 35 and 37.** A mixture of Boc-protected compound (1 equiv., 1 mmol, compounds **36** for **35** and **38** for **37**) in dioxane (4 mL) and hydrochloric acid 37% (2 mL) was stirred at 40 °C for 1 h and then evaporated. The resulting products were obtained in sufficient purity.

**4.1.2.2. Compounds 9 and 12.** A mixture of the 1,2,4-triazole-3-thione compound **8** (1 equiv., 0.2 mmol, 51 mg) and benzoyl chloride (compound **9**) or *p*-tosyl chloride (compound **12**) (1.1 equiv., 0.22 mmol) in DMF was stirred at room temperature for 1 h. The solution was then diluted in EtOAc (10 mL) and washed with water (5x20 mL). The organic layer was dried over MgSO<sub>4</sub>, filtered and evaporated. The crude products were purified on silica gel column (EtOAc/Hex) to yield the corresponding acylated compounds **9** and **12**.

**4.1.2.3. Compounds 10 and 11.** A mixture of the 1,2,4-triazole-3-thione compound **8** (1 equiv., 1 mmol, 257 mg) and phthalic anhydride (1.5 equiv., 1.5 mmol, 222 mg) in pyridine (2 mL) was refluxed for 1 h. The solution was then diluted in EtOAc (20 mL) and washed with water (4x30 mL). The organic layer was dried over MgSO<sub>4</sub>, filtered and evaporated to give a crude powder. The resulting phthalimide **10** was purified by recrystallization from a mixture of EtOAc-Hexane.

A solution of the phthalimide **10** (1 equiv., 0.2 mmol, 70 mg) in a mixture of EtOH-H<sub>2</sub>O (2–1/6 mL) was added to a solution of KOH (112 mg, 10 equiv., 2 mmol) and the reaction was stirred at room temperature for 1 h. The mixture was acidified by an 1 N aqueous solution of KHSO<sub>4</sub> (5 mL) and extracted by EtOAc (3x10 mL). The combined organic layers were dried over MgSO<sub>4</sub>, filtered and evaporated to give a crude powder. Recrystallisation from EtOAc led to the pure compound **11**.

**4.1.2.4. Compound 15.** This compound was obtained from compound **8** and benzohydrazide by following the general synthetic procedure for 1,2,4-triazole-3-thiones.. **4.1.2.6. Compound 39.** A solution of the amino acid compound **37** (1 equiv., 0.2 mmol, 58 mg) and phenyl isocyanate (0.9

equiv., 0.18 mmol., 19 µL) in a mixture of dioxane (4 mL), AcOEt (4 mL) and triethylamine (1 mL) was stirred at room temperature for 2 h. The solution was diluted in water (10 mL) and washed with EtOAc (15 mL). The aqueous layer was lyophilized and the crude product was purified by preparative reverse phase HPLC to give the corresponding urea compound **39**.

## 4.2. Biology

### 4.2.1. Metallo-β-Lactamase inhibition assays

**4.2.1.1. VIM-type enzymes, NDM-1 and IMP-1.** The inhibition potency of the compounds has been assessed as previously reported [38,43]. Briefly, the rate of hydrolysis of a reporter substrate, either 150 µM imipenem or meropenem (λ, 300 nm), 120 µM cefotaxime (λ, 260 nm) or 100 µM nitrocefin (λ, 482 nm), by a purified MBL enzyme (VIM-1, VIM-2, VIM-4, NDM-1, and IMP-1; enzyme concentration in the assay ranged 1–70 nM) was measured at 30 °C in 50 mM HEPES buffer (pH 7.5) in the absence and presence of several concentrations of the inhibitor (0.5 µM –1 mM).

The inhibition constants ( $K_i$ ) were determined on the basis of a model of competitive inhibition by analysing the dependence of the ratio  $v_0/v_i$  ( $v_0$ , hydrolysis velocity in the absence of inhibitor;  $v_i$ , hydrolysis velocity in the presence of inhibitor) as a function of [I] as already described [53]. The assays were performed in triplicate.

**4.2.1.2. L1.** Inhibition assay was performed as previously described [38,43]. Briefly, L1 (0.2–0.8 nM) was tested in 25 mM HEPES pH 7.5 with 50 µM ZnCl<sub>2</sub>. The enzyme and the inhibitor (100 µM) were pre-incubated for 30 min at 21 °C and then incubated at 30 °C in the presence of 100 µM nitrocefin as the reporter substrate ( $\Delta\epsilon^{482} = 15,000 \text{ M}^{-1} \cdot \text{cm}^{-1}$ ). In the present study, no compound inhibited L1 with a residual activity < 30%, and therefore no  $K_i$  was measured [24]. The assays were performed in triplicate.

### 4.2.2. Microbiological assays

The ability of selected compounds to restore the susceptibility of resistant bacteria to a β-lactam antibiotic was assessed as previously described [38,43], according to the CLSI (Clinical Laboratory Standard Institute) recommendations [54,55].

Assays using the agar disk-diffusion method were performed on MBL-producing isogenic laboratory strains obtained after transforming *Escherichia coli* AS19 [56] and LZ2310 [57] strains with a derivative of the high copy number plasmid pLB-II carrying the cloned *bla*<sub>VIM-2</sub> gene. After 18 h incubation at 35 °C in the presence of cefoxitin (30 µg)-containing disks supplemented with an inhibitor or DMSO or EDTA (220 µg) as negative and positive controls, respectively, the diameter of the growth inhibition zone was measured and compared to that obtained in the absence of inhibitor. Experiments were performed in triplicate.

The minimum inhibitory concentration (MICs) of meropenem (MEM) was determined in triplicate using Mueller-Hinton broth (MHB) and a bacterial inoculum of  $5 \times 10^4$  CFU/well, in both the absence and presence of a fixed concentration (32 µg/mL) of an inhibitor. Two multidrug-resistant *K. pneumoniae* isolates producing VIM-1 (7023) and VIM-4 (VA-416/02) and present in our collection were used [58,59].

### 4.2.3. Cytotoxicity assays

The potential cytotoxic activity of selected compounds (**26**, **27** and **60**) was evaluated using the commercially available membrane integrity assay (CytoTox 96® non-radioactive cytotoxicity assay, Promega, Madison, WI, U.S.A.). HeLa cells were grown in Dulbecco's Modified Eagle's Medium (Euroclone, Pero, Italy) supplemented with 10% fetal bovine serum, 4.5 mg/mL glucose and 2 mM L-glutamine (37 °C, 5% CO<sub>2</sub>). The compounds were tested for their ability to induce cell lysis by measuring the release of lactate dehydrogenase (LDH) after incubating



HeLa cell cultures (20,000 cells/well) for 24 h (medium as above, 37 °C, 5% CO<sub>2</sub>) in the absence and presence of varying concentrations of the compound (up to 500 μM). Further controls included samples containing the medium only, 1% DMSO or in which cell lysis was induced by the addition of 9% Triton X-100 (maximum LDH release control). The assay was performed in triplicate.

#### 4.3. Isothermal titration calorimetry (ITC) analysis of compound binding to VIM-2

ITC titration was performed on a MicroCal ITC200 (GE-Malvern) equipped with a 200 μL Hastelloy sample cell and an automated 40 μL glass syringe rotating at 1000 rpm. VIM-2 in 10 mM HEPES-NaOH, 0.15 M NaCl, 50 μM ZnSO<sub>4</sub>, pH 7.5 was diluted to the desired concentration with the same buffer and was brought to DMSO concentration identical to that of the injected compound. The tested compound was solubilized in DMSO at 20 mM concentration and was diluted to 200 μM with the enzyme buffer, resulting in a final DMSO concentration of 1%.

In a standard experiment, VIM-2 (19 μM) was titrated by one initiating injection (0.5 μL) followed by 19 injections (2 μL) of compound 3 (200 μM) at an interval of 150 s. Dilution heat of compound injections into buffer, at the corresponding DMSO concentration, were subtracted from raw data.

The data so obtained were fitted via the non-linear least squares minimization method to determine binding stoichiometry (*n*), association constant (*K<sub>a</sub>*), and change in enthalpy of binding ( $\Delta H^\circ_b$ ) using ORIGIN 7 software v.7 (OriginLab). In the fitting procedure, the compound concentration was lowered in order to provide *n* around 1 and to take compound solubility into account under ITC conditions. The Gibbs free energy of binding,  $\Delta G^\circ_b$ , was calculated from *K<sub>a</sub>* ( $\Delta G^\circ_b = -RT \ln K_a$ ) and the entropic term,  $T\Delta S^\circ_b$ , was derived from the Gibbs-Helmholtz equation using the experimental  $\Delta H^\circ_b$  value ( $\Delta G^\circ_b = \Delta H^\circ_b - T\Delta S^\circ_b$ ).

#### 4.4. Molecular modelling

The docking studies were performed with AutoDock 4.2.6 [60] as previously described [43]. For each ligand, free rotations were defined. Files for the docking were prepared from: (i) the structure of complex VIM-2/JMV4690 (PDB code 6YRP) [38] (the protein was protonated with Dockprep module of Chimera and the program was let to itself protonate His residues, while checking the absence of conflict in the H-bond network); (ii) compounds and protein pdbqt files prepared with AutoDockTools (ADT) [61]. For the protein, seven side-chains were allowed to move: Phe61, Asp62, Tyr67, Asp119, Glu149, Arg228 and Asn233 (to visualize them, see Figure S1).

Molecular graphics and analyses were performed with UCSF Chimera, developed by the Resource of Biocomputing, Visualization and Informatics at the University of California, San Francisco, with support from NIH P41-GM103311.

#### Declaration of Competing Interest

The authors declare no competing financial interest.

#### Acknowledgments

Part of this work was supported by Agence Nationale de la Recherche (ANR-14-CE16-0028-01, including fellowship to L.S.). We thank Mr Pierre Sanchez for mass spectrometry analyses. Thanks are also due to Prof. Liam Good (Royal Veterinary College, London, U.K.) and Prof. Lynn Zechiedrich (Baylor College of Medicine, Houston, USA) for providing the *E. coli* strains AS19 and LZ2310, respectively. We are extremely grateful to Prof. Martti Vaara (Northern Antibiotics Ltd., Espoo, Finland) for providing compound NAB741.

#### Appendix A. Supplementary material

Supplementary data to this article can be found online at <https://doi.org/10.1016/j.bioorg.2021.105024>.

#### References

- [1] C. Lee Ventola, The antibiotic resistance crisis: part1: causes and threats, *Pharm. Ther.* 40 (2015) 277–283. [PMC4378521](https://doi.org/10.1016/j.pharmthera.2015.04.001).
- [2] World Health Organization, Global priority list of antibiotic-resistant bacteria to guide research, discovery and development of new antibiotics, 27 february 2017.
- [3] P. Nordmann, T. Naas, L. Poirel, Global spread of carbapenemase-producing Enterobacteriaceae, *Emerg. Infect. Dis.* 17 (2011) 1791–1798. <https://doi.org/10.3201/eid1710.110655>.
- [4] T.R. Walsh, M.A. Toleman, The emergence of pan-resistant Gram-negative pathogens merits a rapid global political response, *J. Antimicrob. Chemother.* 67 (2012) 1–3. <https://doi.org/10.1093/jac/dkr378>.
- [5] W.C. Reygaert, An overview of the antimicrobial resistance mechanisms of bacteria, *AIMS Microbiol.* 4 (2018) 482–501. <https://doi.org/10.3934/microbiol.2018.3.482>.
- [6] A. Cassini, L.D. Högberg, D. Plachouras, A. Quattrocchi, A. Hoxha, G.S. Simonsen, M. Colomb-Cotinat, M.E. Kretzschmar, B. Devleeschauwer, M. Cecchini, D. A. Ouakrim, T.C. Oliveira, M.J. Struelens, C. Suetens, D.L. Monnet, Burden of AMR Collaborative Group, Attributable deaths and disability-adjusted life-years caused by infections with antibiotic-resistant bacteria in the EU and the European Economic Area in 2015: a population-level modelling analysis, *Lancet Infect. Dis.* 19 (2019) 56–66. [https://doi.org/10.1016/S1473-3099\(18\)30605-4](https://doi.org/10.1016/S1473-3099(18)30605-4).
- [7] K. Bush, Past and present perspectives on  $\beta$ -lactamases, *Antimicrob. Agents Chemother.* 62 (2018) e01076–18. <https://doi.org/10.1128/AAC.01076-18>.
- [8] T. Palzkill, Metallo- $\beta$ -lactamase structure and function, *Ann. N. Y. Acad. Sci.* 1277 (2013) 91–104. <https://doi.org/10.1111/j.1749-6632.2012.06796.x>.
- [9] V.R. Gajamer, B. Bhattacharjee, D. Paul, C. Deshmukhya, A.K. Singh, N. Pradhan, H.K. Tiwari, *Escherichia coli* encoding bla<sub>NDM-5</sub> associated with community-acquired urinary tract infections with unusual MIC creep-like phenomenon against imipenem, *J. Glob. Antimicrob. Resist.* 14 (2018) 228–232. <https://doi.org/10.1016/j.jgar.2018.05.004>.
- [10] S.E. Boyd, D.M. Livermore, D.C. Hooper, W.W. Hope, Metallo- $\beta$ -lactamases: structure, function, epidemiology, treatment options, and the development pipeline, *Antimicrob. Agents Chemother.* 64 (2020) e00397–20. <https://doi.org/10.1128/AAC.00397-20>.
- [11] C. Gonzalez-Bello, D. Rodriguez, M. Pernas, A. Rodriguez, E. Colchon,  $\beta$ -Lactamase inhibitors to restore the efficacy of antibiotics against superbugs, *J. Med. Chem.* 63 (2020) 1859–1881. <https://doi.org/10.1021/acs.jmedchem.9b01279>.
- [12] J.-D. Docquier, S. Mangani, An update on  $\beta$ -lactamase inhibitor discovery and development, *Drug Resist. Updat.* 36 (2018) 13–29. <https://doi.org/10.1016/j.drup.2017.11.002>.
- [13] C.J. Burns, D. Daigle, B. Liu, D. McGarry, D.C. Pevear, R.E. Trout,  $\beta$ -Lactamase inhibitors. WO Patent WO 2014/089365 A1.
- [14] A. Krajnc, J. Brem, P. Hinchliffe, K. Calvopiña, T.D. Panduwawala, P.A. Lang, J.J. A.G. Kamps, J.M. Tyrrell, E. Widlake, B.G. Saward, T.R. Walsh, J. Spencer, C. J. Schofield, Bicyclic boronate VNRX-5133 inhibits metallo- and serine  $\beta$ -lactamases, *J. Med. Chem.* 62 (2019) 8544–8556. <https://doi.org/10.1021/acs.jmedchem.9b00911>.
- [15] B. Liu, R.E.L. Trout, G.H. Chu, D. McGarry, R.W. Jackson, J.C. Hamrick, D. M. Daigle, S.M. Cusick, C. Pozzi, F. De Luca, M. Benvenuti, S. Mangani, J.-D. Docquier, W.J. Weis, D.C. Pevear, L. Xerri, C.J. Burns, Discovery of Taniborbactam (VNRX-5133): a broad spectrum serine- and metallo- $\beta$ -lactamase inhibitor for carbapenem-resistant bacterial infections, *J. Med. Chem.* 63 (2020) 2789–2801. <https://doi.org/10.1021/acs.jmedchem.9b01518>.
- [16] J.C. Vazquez-Ucha, J. Arca-Suarez, G. Bou, A. Beceiro, New carbapenemase inhibitors : clearing the way for the  $\beta$ -lactams, *Int. J. Mol. Sci.* 21 (2020) 9308. <https://doi.org/10.3390/ijms21239308>.
- [17] M. Everett, N. Sprynski, A. Coelho, J. Castandet, M. Bayet, J. Bougnon, C. Lozano, D.T. Davies, S. Leiris, M. Zalacain, I. Morrissey, S. Magnet, K. Holden, P. Warn, F. De Luca, J.-D. Docquier, M. Lemonnier, Discovery of a novel metallo- $\beta$ -lactamase that potentiates meropenem activity against carbapenem-resistant Enterobacteriaceae, *Antimicrob. Agents Chemother.* 62 (2018) e00074–18. <https://doi.org/10.1128/AAC.00074-18>.
- [18] S. Leiris, A. Coelho, J. Castandet, M. Bayet, C. Lozano, J. Bougnon, J. Bousquet, M. Everett, M. Lemonnier, N. Sprynski, M. Zalacain, T.D. Pallin, M.C. Cramp, N. Jennings, G. Raphy, M.W. Jones, R. Pattipati, B. Shankar, R. Sivasubrahmanyam, A.K. Soodhagani, R.R. Juvenhala, N. Pottabathini, S. Pothukanuri, M. Benvenuti, C. Pozzi, S. Mangani, F. De Luca, G. Cerboni, J.-D. Docquier, D.T. Davies, SAR studies leading to the identification of a novel series of metallo- $\beta$ -lactamase inhibitors for the treatment of carbapenem-resistant Enterobacteriaceae infections that display efficacy in an animal infection model, *ACS Infect. Dis.* 5 (2019) 131–140. <https://doi.org/10.1021/acsinfecdis.8b00246>.
- [19] N. Reddy, M. Shungube, P.I. Arvidsson, S. Baijnath, H.G. Kruger, T. Govender, T. Naicker, A 2018–2019 patent review of metallo- $\beta$ -lactamase inhibitors, *Exp. Opin. Ther. Pat.* 30 (2020) 541–555. <https://doi.org/10.1080/13543776.2020.1767070>.
- [20] R.P. McGeary, D.T. Tan, G. Schenk, Progress toward inhibitors of metallo- $\beta$ -lactamases, *Future Med. Chem.* 9 (2017) 673–691. <https://doi.org/10.4155/fmc-2017-0007>.

- [21] A.R. Palacios, M.-A. Rossi, G.S. Mahler, A.J. Vila, Metallo- $\beta$ -lactamase inhibitors inspired on snapshots from the catalytic mechanism, *Biomolecules* 10 (2020) 854, <https://doi.org/10.3390/biom10060854>.
- [22] A.Y. Chen, R.N. Adamek, B.L. Dick, C.V. Credille, C.N. Morrison, S.M. Cohen, Targeting metalloenzymes for therapeutic intervention, *Chem. Rev.* 119 (2019) 1323–1455, <https://doi.org/10.1021/acs.chemrev.8b00201>.
- [23] B.M. Liénard, G. Garau, L. Horsfall, A.I. Karsiotis, C. Dambon, P. Lassaux, C. Papamichael, G.C. Roberts, M. Galleni, O. Dideberg, J.-M. Frère, C.J. Schofield, Structural basis for the broad-spectrum inhibition of metallo- $\beta$ -lactamases by thiols, *Org. Biomol. Chem.* 6 (2008) 2282–2294, <https://doi.org/10.1039/b802311e>.
- [24] P. Lassaux, M. Hamel, M. Gulea, H. Delbrück, P.S. Mercuri, L. Horsfall, D. Dehareng, M. Kupper, J.-M. Frère, K. Hoffmann, M. Galleni, C. Bebrone, Mercaptophosphonate compounds as broad-spectrum inhibitors of the metallo- $\beta$ -lactamases, *J. Med. Chem.* 53 (2010) 4862–4876, <https://doi.org/10.1021/jm100213c>.
- [25] M.M. Gonzalez, M. Kosmopoulou, M.F. Mojica, V. Castillo, P. Hinchliffe, I. Pettinati, J. Brem, C.J. Schofield, G. Mahler, R.A. Bonomo, L.I. Llarull, J. Spencer, A.J. Vila, Bisthiazolidines: a substrate-mimicking scaffold as an inhibitor of the NDM-1 carbapenemase, *ACS Inf. Dis.* 1 (2015) 544–554, <https://doi.org/10.1021/acsinfecdis.5b00046>.
- [26] J.H. Toney, G.G. Hammond, P.M. Fitzgerald, N. Sharma, J.M. Balkovec, G. P. Rouen, S.H. Olson, M.L. Hammond, M.L. Greenlee, Y.D. Gao, Succinic acids as potent inhibitors of plasmid-borne IMP-1 metallo- $\beta$ -lactamase, *J. Biol. Chem.* 276 (2001) 31913–31918, <https://doi.org/10.1074/jbc.M104742200>.
- [27] A.Y. Chen, P.W. Thomas, A.C. Stewart, A. Bergstrom, Z. Cheng, C. Miller, C. R. Bethel, S.H. Marshall, C.V. Credille, C.L. Riley, R.C. Page, R.A. Bonomo, M. W. Crowder, D.L. Tierney, W. Fast, S.M. Cohen, Dipicolinic acid derivatives as inhibitors of New Delhi Metallo- $\beta$ -lactamase-1, *J. Med. Chem.* 60 (2017) 7267–7283, <https://doi.org/10.1021/acs.jmedchem.7b00407>.
- [28] A.M. King, S.A. Reid-Yu, W. Wang, D.T. King, G. De Pascale, N.C. Strynadka, T. R. Walsh, B.K. Coombes, G.D. Wright, Aspergillomarasmine A overcomes metallo- $\beta$ -lactamase antibiotic resistance, *Nature* 510 (2014) 503–506, <https://doi.org/10.1038/nature13445>.
- [29] A. Bergstrom, A. Katko, Z. Adkins, J. Hill, Z. Cheng, M. Burnett, H. Yang, M. Aitha, M.R. Mehaffey, J.S. Brodbelt, K.H. Tehrani, N.I. Martin, R.A. Bonomo, R.C. Page, D. L. Tierney, W. Fast, G.D. Wright, M.W. Crowder, Probing the interaction of aspergillomarasmine A with metallo- $\beta$ -lactamase NDM-1, VIM-2, and IMP-7, *ACS Infect. Dis.* 4 (2018) 135–145, <https://doi.org/10.1021/acsinfecdis.7b00106>.
- [30] A. Matsuura, H. Okumura, R. Asakura, N. Ashizawa, M. Takahashi, F. Kobayashi, N. Ashikawa, K. Arai, Pharmacological profiles of aspergillomarasmies as endothelin converting enzyme inhibitors, *Jpn J. Pharmacol.* 63 (1993) 187–193, <https://doi.org/10.1254/jpp.63.187>.
- [31] O. Samuelsen, O.A.H. Astrand, C. Fröhlich, A. Heikal, S. Skagseth, T.J.O. Carlsen, H.S. Leiros, A. Bayer, C. Schnaars, G. Kildahl-Andersen, S. Lauksund, S. Finke, S. Huber, T. Gjoen, A.M.S. Andresen, O.A. Okstad, ZN148 – a modular synthetic metallo- $\beta$ -lactamase inhibitor reverses carbapenem-resistance in Gram-negative pathogens in vivo, *Antimicrob. Agents Chemother.* 64 (2020) e02415–19, <https://doi.org/10.1128/AAC.02415-19>.
- [32] J. Brem, R. Cain, S. Cahill, M.A. McDonough, I.J. Clifton, J.C. Jiménez-Castellanos, M.B. Avison, J. Spencer, C.W. Fishwick, C.J. Schofield, Structural basis of metallo- $\beta$ -lactamase, serine- $\beta$ -lactamase and penicillin-binding protein inhibition by cyclic boronates, *Nat. Commun.* 7 (2016) 12406, <https://doi.org/10.1038/ncomms12406>.
- [33] S.J. Hecker, K.R. Reddy, O. Lomovskaya, D.C. Griffith, D. Rubio-Aparicio, K. Nelson, R. Tsvikovski, D. Sun, M. Sabet, Z. Tarazi, J. Parkinson, M. Totrov, S. H. Boyer, T.W. Glinka, O.A. Pemberton, Y. Chen, M.N. Dudley, Discovery of cyclic boronic acid QPX7728, an ultra-broad-spectrum inhibitor of serine and metallo- $\beta$ -lactamases, *J. Med. Chem.* 63 (2020) 7491–7507, <https://doi.org/10.1021/acs.jmedchem.9b01976>.
- [34] L. Olsen, S. Jost, H.W. Adolph, I. Pettersson, L. Hemmingsen, F.S. Jørgensen, New leads of metallo- $\beta$ -lactamase inhibitors from structure-based pharmacophore design, *Bioorg. Med. Chem.* 14 (2006) 2627–2635, <https://doi.org/10.1016/j.bmc.2005.11.046>.
- [35] K. Kwapien, M. Damergi, S. Nader, L. El Khoury, Z. Hobaika, R.G. Maroun, J.-P. Piquemal, L. Gavara, D. Berthomieu, J.-F. Hernandez, N. Gresh, Calibration of 1,2,4-triazole-3-thione, an original Zn-binding group of metallo- $\beta$ -lactamase inhibitors. Validation of a polarizable MM/MD potential by quantum chemistry, *J. Phys. Chem. B* 121 (2017) 6295–6312, <https://doi.org/10.1021/acs.jpcc.7b01053>.
- [36] L. Nauton, R. Kahn, G. Garau, J.-F. Hernandez, O. Dideberg, Structural insights into the design of inhibitors of the L1 metallo- $\beta$ -lactamase from *Stenotrophomonas maltophilia*, *J. Mol. Biol.* 375 (2008) 257–269, <https://doi.org/10.1016/j.jmb.2007.10.036>.
- [37] T. Christopeit, T.J. Carlsen, R. Helland, H.K. Leiros, Discovery of novel inhibitor scaffolds against the metallo- $\beta$ -lactamase VIM-2 by surface plasmon resonance (SPR) based fragment screening, *J. Med. Chem.* 58 (2015) 8671–8682, <https://doi.org/10.1021/acs.jmedchem.5b01289>.
- [38] L. Gavara, L. Seville, F. De Luca, P. Mercuri, C. Bebrone, G. Feller, A. Legru, G. Cerboni, S. Tanfoni, D. Baud, G. Cutolo, B. Bestgen, G. Chelini, F. Verdirosa, F. Sannio, C. Pozzi, M. Benvenuti, K. Kwapien, M. Fischer, K. Becker, J.-M. Frère, S. Mangani, N. Gresh, D. Berthomieu, M. Galleni, J.-D. Docquier, J.-F. Hernandez, 4-Amino-1,2,4-triazole-3-thione-derived Schiff bases as metallo- $\beta$ -lactamase inhibitors, *Eur. J. Med. Chem.* 208 (2020), 112720, <https://doi.org/10.1016/j.ejmech.2020.112720>.
- [39] F. Spyarakis, M. Santucci, L. Maso, S. Cross, E. Gianquinto, F. Sannio, F. Verdirosa, F. De Luca, J.-D. Docquier, L. Cendron, D. Tondi, A. Venturelli, G. Cruciani, M. P. Costi, Virtual screening identifies broad-spectrum  $\beta$ -lactamase inhibitors with activity on clinically relevant serine- and metallo-carbapenemases, *Sci. Rep.* 10 (2020) 12763, <https://doi.org/10.1038/s41598-020-69431-y>.
- [40] P. Vella, W.M. Hussein, E.W. Leung, D. Clayton, D.L. Ollis, N. Mitić, G. Schenk, R. P. McGeary, The identification of new metallo- $\beta$ -lactamase inhibitor leads from fragment-based screening, *Bioorg. Med. Chem. Lett.* 21 (2011) 3282–3285, <https://doi.org/10.1016/j.bmcl.2011.04.027>.
- [41] F. Spyarakis, G. Celenza, F. Marcoccia, M. Santucci, S. Cross, P. Bellio, L. Cendron, M. Perilli, D. Tondi, Structure-based virtual screening for the discovery of novel inhibitors of New Delhi Metallo- $\beta$ -lactamase-1, *ACS Med. Chem. Lett.* 9 (2017) 45–50, <https://doi.org/10.1021/acsmedchemlett.7b00428>.
- [42] L. Seville, L. Gavara, C. Bebrone, F. De Luca, L. Nauton, M. Achard, P. Mercuri, S. Tanfoni, L. Borgianni, C. Guyon, P. Lonjon, G. Turan-Zitouni, J. Dzieciolowski, K. Becker, L. Bénard, C. Condon, L. Maillard, J. Martinez, J.-M. Frère, O. Dideberg, M. Galleni, J.-D. Docquier, J.-F. Hernandez, 1,2,4-Triazole-3-thione compounds as inhibitors of dizinc metallo- $\beta$ -lactamase, *ChemMedChem* 12 (2017) 972–985, <https://doi.org/10.1002/cmdc.201700186>.
- [43] L. Gavara, F. Verdirosa, A. Legru, P.S. Mercuri, L. Nauton, L. Seville, G. Feller, D. Berthomieu, F. Sannio, F. Marcoccia, S. Tanfoni, F. De Luca, N. Gresh, M. Galleni, J.-D. Docquier, J.-F. Hernandez, 4-(N-Alkyl- and -acyl-amino)-1,2,4-triazole-3-thione analogs as metallo- $\beta$ -lactamase inhibitors: impact of 4-linker on potency and spectrum of inhibition, *Biomolecules* 10 (2020) 1094, <https://doi.org/10.3390/biom10081094>.
- [44] R.F. Deprez-Poulain, J. Charton, V. Leroux, B.P. Deprez, Convenient synthesis of 4H-1,2,4-triazole-3-thiols using di-2-pyridylthionocarbamate, *Tetrahedron Lett.* 48 (2007) 8157–8162, <https://doi.org/10.1016/j.tetlet.2007.09.094>.
- [45] M. Masi, M. Réfreigiers, K.M. Pos, J.-M. Pagès, Mechanisms of envelope permeability and antibiotic influx and efflux in Gram-negative bacteria, *Nat. Microbiol.* 2 (2017) 17001, <https://doi.org/10.1038/nmicrobiol.2017.1>.
- [46] E. Freire, Do enthalpy and entropy distinguish first class from best in class? *Drug Discov. Today* 13 (2008) 869–874, <https://doi.org/10.1016/j.drudis.2008.07.005>.
- [47] J.E. Ladbury, Calorimetry as a tool for understanding biomolecular interactions and an aid to drug design, *Biochem. Soc. Trans.* 38 (2010) 888–893, <https://doi.org/10.1042/BST0380888>.
- [48] L. Borgianni, J. Vandenameele, A. Matagne, L. Bini, R. Bonomo, J.-M. Frère, G. M. Rossolini, J.-D. Docquier, Mutational analysis of VIM-2 reveals an essential determinant for metallo- $\beta$ -lactamase stability and folding, *Antimicrob. Agents Chemother.* 54 (2010) 3197–3204, <https://doi.org/10.1128/AAC.01336-09>.
- [49] R.P. Lamers, J.F. Cavallari, L.L. Burrows, The efflux inhibitor phenylalanine-arginine-naphthylamide (PAN) permeabilizes the outer membrane of gram-negative bacteria, *PLoS one* 8 (2013), e60666, <https://doi.org/10.1371/journal.pone.0060666>.
- [50] M. Vaara, Novel derivatives of polymyxins, *J. Antimicrob. Chemother.* 68 (2013) 1213–1219, <https://doi.org/10.1093/jac/dkt039>.
- [51] M. Vaara, Polymyxin derivatives that sensitize Gram-negative bacteria to other antibiotics, *Molecules* 24 (2019) 249, <https://doi.org/10.3390/molecules24020249>.
- [52] E.F. Pettersen, T.D. Goddard, C.H. Huang, G.S. Couch, D.M. Greenblatt, E.C. Meng, T.E. Ferrin, U.C.S.F. Chimera, a visualization system for exploratory research and analysis, *J. Comput. Chem.* 25 (2004) 1605–1612, <https://doi.org/10.1002/jcc.20084>.
- [53] J.-D. Docquier, J. Lamotte-Brasseur, M. Galleni, G. Amicosante, J.M. Frère, G. M. Rossolini, On functional and structural heterogeneity of VIM-type metallo- $\beta$ -lactamases, *J. Antimicrob. Chemother.* 51 (2003) 257–266, <https://doi.org/10.1093/jac/dkg067>.
- [54] Clinical Laboratory Standard Institute, Performance standards for antimicrobial disk susceptibility tests; approved standard, Document M02-A12, 2015, Twelfth Edition, Wayne, PA, USA.
- [55] Clinical Laboratory Standard Institute, Methods for dilution antimicrobial susceptibility tests for bacteria that grow aerobically, Document M07-A10, 2015, Twelfth Edition, Wayne, PA, USA.
- [56] M. Avalos, M. Boetzer, W. Pirovano, N.E. Arenas, S. Douthwaite, G.P. van Wezel, Complete genome sequence of *Escherichia coli* AS19, an antibiotic-sensitive variant of *E. coli* strain B REL606, *Genome Announc.* 6 (2018) e00385-18, <https://doi.org/10.1128/genomeA.00385-18>. DOI: .
- [57] S. Yang, S.R. Clayton, E.L. Zechiedrich, Relative contributions of the AcrAB, MdfA and NorE efflux pumps to quinolone resistance in *Escherichia coli*, *J. Antimicrob. Chemother.* 51 (2003) 545–556, <https://doi.org/10.1093/jac/dkg126>.
- [58] S. Cagnacci, L. Gualco, S. Roveta, S. Mannelli, L. Borgianni, J.-D. Docquier, F. Dodi, M. Centanaro, E. Debbia, A. Marchese, G.M. Rossolini, Bloodstream infections caused by multidrug-resistant *Klebsiella pneumoniae* producing the carbapenem-hydrolysing VIM-1 metallo- $\beta$ -lactamase: first Italian outbreak, *J. Antimicrob. Chemother.* 61 (2008) 296–300, <https://doi.org/10.1093/jac/dkm471>.
- [59] F. Luzzaro, J.-D. Docquier, C. Colino, A. Endimiani, G. Lombardi, G. Amicosante, G.M. Rossolini, A. Toniolo, Emergence in *Klebsiella pneumoniae* and *Enterobacter cloacae* clinical isolates of the VIM-4 metallo- $\beta$ -lactamase encoded by a conjugative plasmid, *Antimicrob. Agents Chemother.* 48 (2004) 648–650, <https://doi.org/10.1128/aac.48.2.648-650.2004>.
- [60] G.M. Morris, R. Huey, W. Lindstrom, M.F. Sanner, R.K. Belew, D.S. Goodsell, A. J. Olson, AutoDock4 and AutoDockTools4: automated docking with selective receptor flexibility, *J. Comput. Chem.* 16 (2009) 2785–2791, <https://doi.org/10.1002/jcc.21256>.
- [61] M.F. Sanner, Python: a programming language for software integration and development, *J. Mol. Graph. Mod.* 17 (1999) 57–61. PMID: 10660911.